Turbulent transport in the solar nebula

By K. W. Thompson

This paper describes the current state of an ongoing project to simulate turbulent flow in a solar nebula, which is the flattened disk of dust and gas out of which a solar system forms. The goal of this project is to determine a model for the transport of mass and angular momentum in the nebula.

The nebula flow exhibits compressibility, thermal conduction, viscosity, internal heating through viscous dissipation, a stable shear due to Keplerian rotation, and a gravitational acceleration in the vertical direction which is linear with altitude. These properties combine to give flow patterns not seen in terrestrial applications.

Primordial solar systems are known to exist and are presumably undergoing an evolution similar to the early stages of our own solar system; for example, the IRAS infrared telescope has discovered such a protoplanetary system around the star Vega. Solar nebula evolution is the subject of much research in the astrophysical community. In the long run, researchers hope to gain a better understanding of planetary formation and the processes which dissipate the solar nebula with time (Black & Matthews (1985)).

1. Background

The solar nebula circled the Sun during and shortly after its formation. The nebula is thought to have formed out of the contraction of a much larger and even more diffuse molecular cloud. The nebula's central star, our Sun, also formed out of the molecular cloud matter, and it is the Sun's gravity which held the nebula together and kept it from flying apart. The combination of the Sun's gravitational field, the initial angular momentum of the molecular cloud (retained by the nebular material), and radiative cooling is believed to have confined the solar nebula to a thin disk, rather than a cloud.

Each fluid element follows a nearly Keplerian orbit around the central star. Consequently, the radial velocity of the gas decreases with increasing orbital radius r, and the nebula undergoes a shear flow. Viscosity causes friction between adjacent rings of fluid and has a braking effect on the inner ring, decreasing its total energy and causing the fluid to spiral in toward the star. The net result is to turn orbital kinetic energy into heat and to drag much of the nebular gas inward, where it ultimately becomes part of the central star. As mass is transported inward, angular momentum is transported outward.

The problem with this scenario is that molecular viscosity is too small to dissipate the nebula in a reasonable amount of time. Other effects must be invoked to explain the disappearance of the nebula, and turbulence is a logical candidate.

Turbulence may act globally much as a large viscosity, mixing fluid elements of different energy and angular momentum and augmenting the transport of mass and angular momentum.

Anticipated sources of turbulence include thermal convection (driven by the heat generated from viscous dissipation), vertical shear in the angular velocity (due to the nonuniform deviations from the central plane orbital motion of the gas with altitude), and the large velocity differential between the rotating disk matter and the infalling (non-Keplerian) molecular cloud material. Of these, turbulent convection is the focus of the current work. Turbulent convection is strongly affected by the compressibility of the flow because the density and pressure vary substantially with altitude above the nebula midplane. Hence, the study of compressible turbulence is central to this project.

The greatest obstacle to the accurate modeling of the solar nebula is the fact that the length scales on which viscous dissipation takes place (and on which the turbulent kinetic energy is turned into heat) is many orders of magnitude smaller than the size of the disk. Consequently, it is not currently possible to create a single computational model which accurately simulates both the large scale structure and the small scale dissipative processes. The objective of this project is to simulate numerically the turbulent processes on a small scale, and to obtain a parameterization of these processes which may be used in other attempts to model the large scale evolution of the nebula.

2. Previous work

The work currently being performed is closely connected with that of Cabot, Hubickyj, and Pollack (hereafter CHP), who have been using the turbulent channel flow code of Kim, Moin, & Moser (1987) to investigate incompressible turbulence in the solar nebula.

The Keplerian flow velocities are highly supersonic in the rest frame of the central star. A direct simulation of the flow in the star's rest frame is impractical, as the flow velocities dictate unworkably small time steps. A better approach is to work in a coordinate system which is comoving with the average flow in the model volume, so that the velocities are subsonic in the model's coordinate system, and the time steps are more reasonable.

CHP have relied upon a coordinate transformation based on the work of Rogallo (1981) to represent the radial shear in a form which permits the use of periodic boundary conditions in the radial direction. The Rogallo transformation eliminates the need to devise boundary conditions which properly advect turbulent flow in and out of the radial boundaries.

In the comoving frame, the gravitational acceleration varies with altitude z above the nebula midplane. The disk is very thin compared to its radial dimensions; therefore a fluid element a distance z above the central disk plane experiences a downward-directed gravitational force (due to the central star) which is proportional to z. This linear variation of gravity has a significant effect on the convective flow. Convection in the Earth's atmosphere takes place in an altitude range over which the gravitational acceleration is essentially constant. The nebular problem has a variable acceleration with altitude, which gives rise to flow patterns not seen in constant gravity environments.

The results of CHP show that those fluid elements above the midplane which are cooler than the average temperature experience a downward acceleration which draws them toward the midplane. Although the acceleration ceases when the fluid reaches the midplane, inertia carries the fluid through the midplane and beyond, until the now-reversed gravitational acceleration robs them of momentum. Thus the zero gravity region experiences some of the most extreme motions, and the variable gravity leads to novel convection patterns.

The computational technique of Kim et al., as currently implemented by CHP, assumes an incompressible fluid. The incompressible approximation is fundamentally flawed for two reasons. First, the density varies significantly with altitude in the real nebula, and fluid elements which move in the vertical direction undergo substantial volume changes. Secondly, the incompressible code uses wall boundary conditions at the vertical boundaries, leading to boundary layer formation, while there are no such boundary layers in the solar nebula. These limitations in turn motivate the current work.

3. Current work

A compressible calculation can overcome the limitations of constant density and boundary layer effects to which an incompressible calculation is subject. Density variations and compressibility are taken care of automatically. The boundary layer problem can be alleviated by adjusting the heating profile to put a nonconvecting layer of fluid next to the walls, so that the convecting flow does not feel the walls directly and cannot form boundary layers. In the event that reflection of acoustic waves from the wall boundaries causes unacceptable perturbations to the interior solution, nonreflecting boundary conditions might be adopted to allow the acoustic waves to propagate out of the calculation, as in Thompson (1987a, 1987b, 1990).

The current work is focused on the simulation of compressible turbulent convection in three dimensions, in which the flow is subjected to a linearly varying gravitational acceleration, viscosity, thermal conduction, and a uniformly applied volume heating. The heat supplied is enough to make the fluid convectively unstable, and convection results. The current problem was formulated to be as much like the corresponding incompressible problem solved CHP as possible, with the goal of comparing the two calculations for consistency. CHP solved this problem by adopting the Boussinesq approximation, in which the flow is assumed to be incompressible and density variations are ignored except for gravitational acceleration (Chandrasekhar (1961)).

4. Numerical method

The equations to be solved are the compressible Navier-Stokes equations. They describe the time evolution of a single compressible fluid in three dimensions, and incorporate the effects of a variable gravitational field, molecular viscosity, thermal conductivity, heating through viscous dissipation, and a separately imposed volume heating.

The current calculations are performed with a code which is designed to conserve mass, energy, and local vorticity. An earlier code which was not conservative was found to become unstable after a sufficient length of time. The conservative code was written in the hope that it would be more stable, and this has proven to be the case.

The density and energy equations are written in conservative form, the conserved energy being the total (= kinetic + thermal + gravitational):

$$\frac{\partial \rho}{\partial t} + \nabla \cdot (\rho \mathbf{u}) = 0,$$

$$\frac{\partial e}{\partial t} + \nabla \cdot [(e + p)\mathbf{u} - \mathbf{u} \cdot \boldsymbol{\sigma} - \kappa \nabla T] = Q,$$

where $e = (1/2)\rho \mathbf{u} \cdot \mathbf{u} + \epsilon + \rho\Phi$; and where ρ is the density, e is the total energy density, Φ is the gravitational potential, $\mathbf{u}$ is the velocity, p is the pressure, T is the temperature, κ is the thermal conductivity, Q is the volume heating rate, $\epsilon = p/(\gamma - 1)$ is the thermal energy density, and $\boldsymbol{\sigma}$ is the viscosity tensor.

Numerical approximations to Eqs. (1–2) can be constructed which exactly conserve the total mass and energy of the system. The numerical conservation laws hold provided that suitable numerical approximations are chosen for both the volume integral of the fields and the spatial derivatives. Such approximations have been constructed, and the calculations verify that the numerical conservation laws are satisfied exactly.

The velocity equations are written in the form

$$\frac{\partial \mathbf{u}}{\partial t} - \mathbf{u} \times \boldsymbol{\omega} + \nabla \left(\frac{1}{2} \mathbf{u} \cdot \mathbf{u} + \frac{\gamma}{\gamma - 1} \frac{p}{\rho} \right) = \mathbf{g} - \frac{1}{(\gamma - 1)\rho} \left(c^2 \nabla \rho - \nabla p \right) + \frac{1}{\rho} \nabla \cdot \boldsymbol{\sigma},$$

where $\boldsymbol{\omega} = \nabla \times \mathbf{u}$ is the vorticity, c is the speed of sound, and $\mathbf{g} = -\nabla\Phi$ is the gravitational acceleration.

The viscosity tensor elements are

$$\sigma_{ij} = \mu \left(\frac{\partial u_i}{\partial x_j} + \frac{\partial u_j}{\partial x_i} - \frac{2}{3} \delta_{ij} \nabla \cdot \mathbf{u} \right),$$

where μ is the viscosity.

The pressure appears in two terms in the velocity equation, rather than as the single pressure gradient term normally seen. The reason for this formulation is to avoid the spurious generation of vorticity by the numerical approximations. Taking the curl of the velocity equation gives

$$\frac{\partial \omega}{\partial t} - \nabla \times (\mathbf{u} \times \boldsymbol{\omega}) = \nabla \times \left[-\frac{1}{(\gamma - 1)\rho} \left(c^2 \nabla \rho - \nabla p \right) + \frac{1}{\rho} \nabla \cdot \boldsymbol{\sigma} \right],$$

because the curl of a gradient is zero.

In the limit of zero viscosity ($\sigma = 0$), the vorticity will remain zero at all times provided that it is zero to begin with and that the fluid is has a spatially constant entropy. (The latter condition implies $c^2 \nabla \rho - \nabla p = 0$.) The numerical approximation to the velocity equation also avoids the spurious generation of vorticity as long as the equation is cast into the form of Eq. (3). Analytically, vorticity is not generated because the curl of the gradient is zero, due to the fact that spatial derivatives commute: $\partial^2 f/\partial x \partial y - \partial^2 f/\partial y \partial x = 0$. The vorticity conservation carries over to the numerical case because the finite difference approximations to x and y derivatives also commute.

The flow is defined to be periodic in the x and y directions. Slip wall (zero stress) and constant temperature conditions are imposed at the z boundaries $z = \pm\delta$. Gravity acts only in the z direction, for which the acceleration is linear in z: $g = -g_w(z/\delta)$, where $g = g_w$ at $z = \delta$. The heating rate Q is uniform throughout the computational volume. The ratio of specific heats is $\gamma = 1.4$.

The spatial derivatives in the above equations are approximated by fourth order finite difference formulas. Suitable one-sided approximations are made at the vertical boundaries at $z = \pm\delta$, while centered approximations are made in the interior. The one-sided approximations are designed to preserve the numerical conservation of mass and energy, and are third order accurate. The complete set of derivative approximations is fourth order accurate.

The time integration is performed by the classic fourth order Runge-Kutta scheme, which is simple to implement and has excellent stability properties. The time dependent solution, therefore, has a global accuracy of fourth order and contains little numerical dissipation. Consequently, the short wavelength solution components do not undergo significant damping due to the numerical scheme.

The choice of an explicit method over an implicit method stems from the need to resolve the smallest features present in the flow. At the smallest length scales, viscosity dominates the evolution of the flow. Since we need to simulate the dissipation of kinetic energy accurately at these scales, the grid spacing and time steps necessary are set by the properties of the flow, and are the same whether explicit or implicit methods are used. The optimal grid spacing and time step are those for which the propagation and viscous Courant numbers are nearly equal. Consequently, the simpler explicit approach has been selected.

5. Results

The flow is characterized by seven numbers. These numbers have been chosen as the scale Mach number M, the Prandtl number Pr (ratio of viscosity to conductivity), the Rayleigh number Ra (related to the volume heating Q), the density exponent α, the scale density ρ_0, the wall gravity g_w, and the wall temperature T_w. The initial state consists of an unstable static solution to which velocity perturbations are added. The temperature and density initially vary with z as $T = T_w + T_s(1 - z^2/\delta^2)$ and $\rho = \rho_0[T/(T_w + T_s)]^{\alpha-1}$, where $T_s = Q\delta^2/(2\kappa)$ is a scale temperature, α is the density exponent, and κ is the thermal conductivity.

The current simulations are defined by $M = 1$, $Pr = 0.2$, $Ra = 1.25 \times 10^5$, $\alpha = 1$, $\rho_0 = 1$, $g_w = 1000$, and $T_w = 300$. The actual flow Mach numbers are ≤ 0.3, and thus approximate an incompressible flow only in a qualitative sense. The Prandtl and Rayleigh numbers are the same as for the incompressible calculations. The density exponent α has no counterpart in the incompressible calculations and was chosen as $\alpha = 1$ to minimize the density variation. With $\alpha = 1$ the density is constant initially, but subsequently assumes an approximately Gaussian distribution with z.

Figure 1 shows the density and temperature profiles for a typical calculation. The plots represent data which is averaged both in time and in the horizontal directions, and then plotted with respect to z. Figures 2 and 3 show the spectra and autocorrelations in the x and y directions at the midplane ($z = 0$).

Figure 1 clearly shows the effects of compressibility on the solution. An incompressible flow responds to a convectively unstable state by undergoing turbulent convection, which redistributes the heat and decreases the temperature gradients from the initial perturbed state. The compressible flow not only redistributes the heat, but also the density, into a more stable distribution. In the isothermal limit where $T = T_c$, the density follows a Gaussian distribution $\rho = \rho_c e^{-z^2/2H^2}$, where $H = \sqrt{kT_c\delta/mg_w}$ is the isothermal scale height, k is Boltzmann's constant, and m is the molecular mass. The convecting flow is not isothermal, but it does exhibit smaller temperature gradients than the initial state, and the density is clearly tending to a Gaussian distribution.

The results agree qualitatively with those of CHP for the analogous incompressible problem, but show some interesting differences as well. Relative to the incompressible results, the compressible results show a higher midplane temperature which is more sharply peaked, and up by a factor of 1.6; and smaller temperature and velocity fluctuations, down by a factor of 0.7. The results should not be expected to agree exactly, as the compressible results show significant density variation, while the incompressible results do not.

6. Future directions

The next task is to study the effects of nonuniform density profiles on turbulent intensities. The current simulations began with a flat density profile in an unstable steady state, which was perturbed to initiate the growth of convection. The time averaged steady state shows a density which resembles a Gaussian

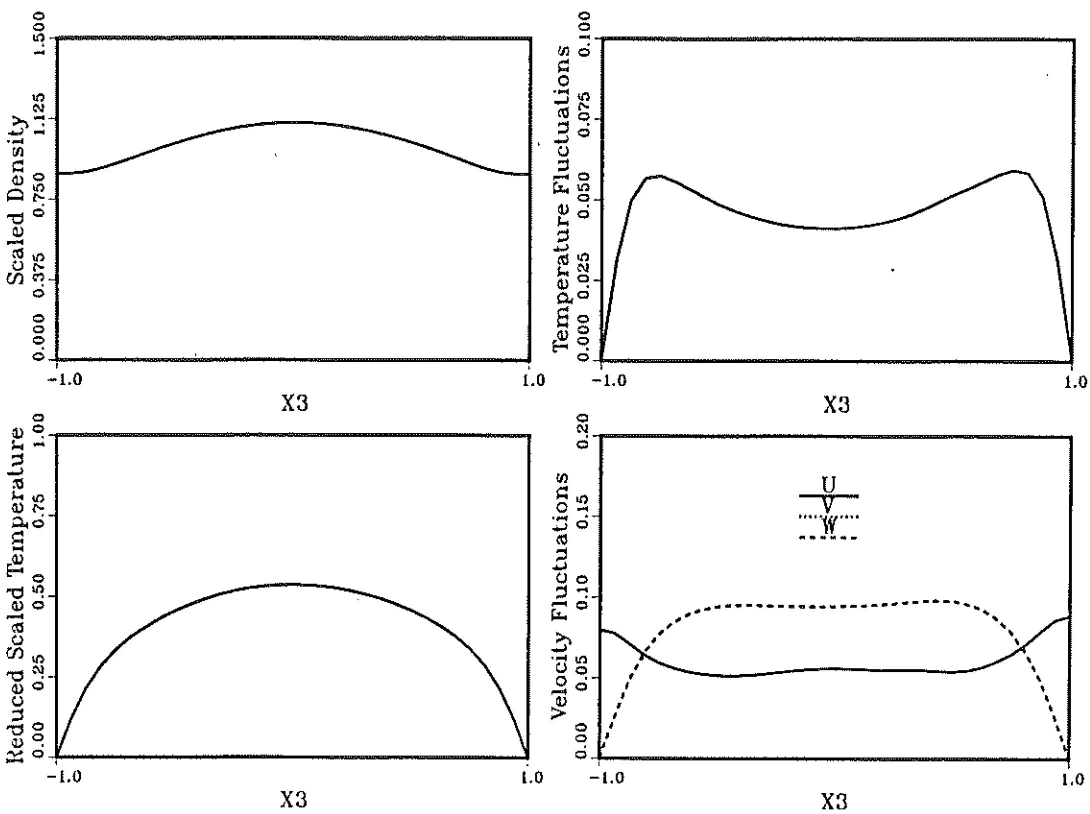

FIGURE 1. Horizontally and temporally averaged solutions for the statistical steady state, plotted versus altitude z. Density is normalized by its initial value. The temperature plot shows $(T - T_w)/T_s$. The RMS temperature and velocity fluctuations about the mean are also shown. Note: V and W curves are identical.

curve, and is peaked at the midplane. Further simulations will begin with an initial density profile which is peaked at the midplane, and should lead to a final state which shows even more density variation. Comparison of these two cases should demonstrate the dependence of turbulent intensities on the density stratification. It will be interesting to see if the incompressible results are approached as a constant density limit of the compressible results.

Some consideration is being given to the incorporation of a compressible sub-grid scale model, such as that of Zeman. Such a model might render the calculations more economical by allowing the use of a coarser grid; currently the calculations take $\approx$ 10 hours of CPU time on a Cray YMP to collect decent statistics for a single set of physical parameters. The current calculations might also serve as a test for the validity of sub-grid scale models.

Subsequent work will evolve the simulations to more accurate approximations

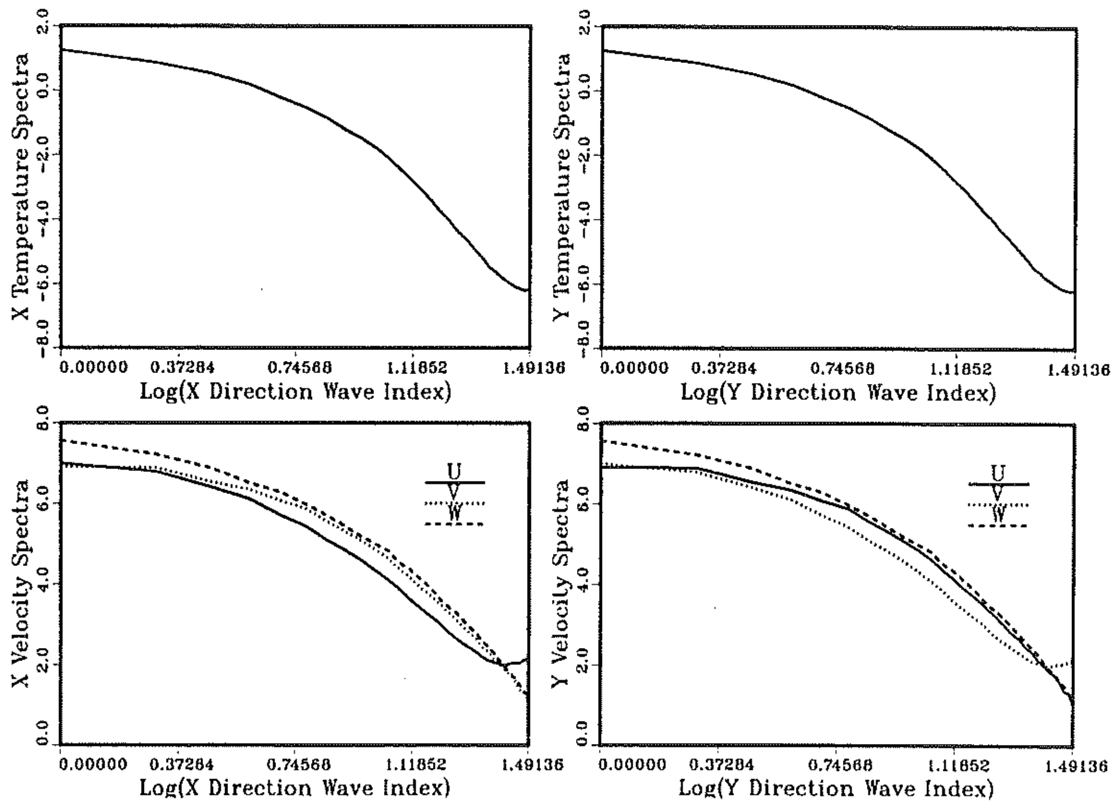

FIGURE 2. Log-log plots of the spectral intensities of the temperature and velocity fluctuations, versus the x and y direction wave numbers, at the midplane ($z = 0$).

of the actual nebula conditions. The stages to be followed will add major new physical phenomena, such as rotation, shear, and radial asymmetry.

The effects of rotation will be included by adopting a rotating coordinate system which is comoving with the flow, and in which the flow is subject to "centrifugal" forces as well as gravitational forces.

The effects of shear will be simulated by assuming a given base flow which is Keplerian, and solving for the nonlinear perturbations with respect to the base flow. The Rogallo transformation of CHP will not be used *per se*, although its useful effects will be duplicated; instead, the perturbations will be assumed to be periodic in a sheared coordinate frame, and will be mapped onto a stationary grid by appropriate coordinate transformations. This approach avoids the distortions entailed by the Rogallo transformation, in which the coordinate grid is itself sheared and must be periodically remapped to a new grid to prevent the grid

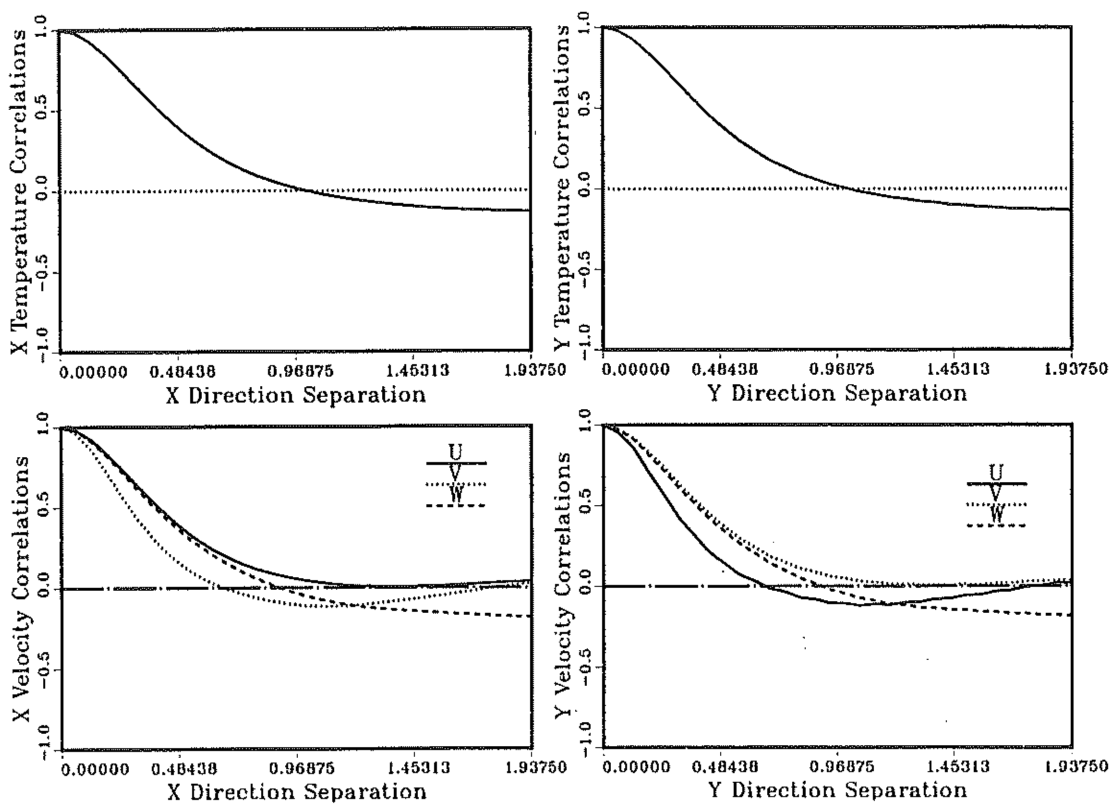

FIGURE 3. Autocorrelations of the temperature and velocity fields, versus x and y direction separations, at the midplane ($z = 0$).

from collapsing.

Radial asymmetry is ultimately required for the flow to result in a net transport of mass and angular momentum in the radial direction. Radial asymmetry renders the flow nonperiodic in the radial direction, prohibiting the use of periodic boundary conditions in this direction. It is not clear at this point how best to implement radial asymmetry. One possibility is to assume that the solution at the inner and outer boundaries consists of a known base state (from the Keplerian profile) plus a perturbation, and to assume that the perturbations at the two boundaries are related by a scaling factor. This issue will require further research.

The results of each of the above modifications will be studied carefully before proceeding to the next. By the time radial asymmetry has been implemented, we should be in a position to answer questions about the effectiveness of turbulence in transporting mass and angular momentum in the solar nebula.

REFERENCES

BLACK, D. C. & MATTHEWS, M. S. (EDITORS) 1985 *Protostars and Planets II*, University of Arizona Press. Tucson, Arizona.

CHANDRASEKHAR, S. 1961 *Hydrodynamic and Hydromagnetic Stability*, Oxford University Press (reprinted by Dover Publications, New York NY).

KIM, J., MOIN, P. & MOSER, R. 1987 Turbulence statistics in fully developed channel flow at low Reynolds number. *Journal of Fluid Mechanics.* **177**, 133.

ROGALLO, R. 1981 *Numerical Experiments in Homogeneous Turbulence*, NASA Technical Memorandum 81315.

THOMPSON, K. W. 1987a Time Dependent Boundary Conditions for Hyperbolic Systems. *Journal of Computational Physics.* **68**, 1.

THOMPSON, K. W. 1987b *Lecture Series in Computational Fluid Dynamics*, NASA Technical Memorandum 10010.

THOMPSON, K. W. 1990 Time Dependent Boundary Conditions for Hyperbolic Systems. II. *Journal of Computational Physics.* To appear.